

# Spatial variability of the hydrochemistry of shallow groundwaters and surface waters of the Rensdyrbekken: A case study of a permafrost catchment in Bellsund (SW Spitsbergen, Svalbard)

Sara Lehmann-Konera<sup>1</sup>  | Piotr Zagórski<sup>1</sup>  | Kamil Nowiński<sup>2</sup> |  
 Krzysztof Raczyński<sup>3</sup>  | Marcin Frankowski<sup>4</sup>  | Łukasz Franczak<sup>1</sup>  |  
 Mateusz Dobek<sup>1</sup>  | Danuta Szumińska<sup>5</sup>  | Marek Ruman<sup>6</sup>  |  
 Ramia Al Bakain<sup>7</sup>  | Żaneta Polkowska<sup>8</sup> 

<sup>1</sup>Faculty of Earth Sciences and Spatial Management, Institute of Earth and Environmental Sciences, Maria Curie-Skłodowska University in Lublin, Lublin, Poland

<sup>2</sup>Laboratory of Limnology, Department of Hydrology, Faculty of Oceanography and Geography, Gdańsk University, Gdańsk, Poland

<sup>3</sup>Geosystems Research Institute, Mississippi State University, Starkville, Mississippi, USA

<sup>4</sup>Department of Analytical and Environmental Chemistry, Faculty of Chemistry, Adam Mickiewicz University in Poznań, Poznań, Poland

<sup>5</sup>Faculty of Geographical Sciences, Kazimierz Wielki University, Bydgoszcz, Poland

<sup>6</sup>Faculty of Natural Sciences, University of Silesia in Katowice, Sosnowiec, Poland

<sup>7</sup>Department of Chemistry, School of Science, The University of Jordan, Amman, Jordan

<sup>8</sup>Department of Analytical Chemistry, Faculty of Chemistry, Gdańsk University of Technology, Gdańsk, Poland

## Correspondence

Sara Lehmann-Konera, Faculty of Earth Sciences and Spatial Management, Institute of Earth and Environmental Sciences, Maria Curie-Skłodowska University in Lublin, 2d Kraśnicka Ave., Lublin 20-718, Poland.  
 Email: [sara.lehmann-konera@mail.umcs.pl](mailto:sara.lehmann-konera@mail.umcs.pl)

Kamil Nowiński, Faculty of Oceanography and Geography, Institute of Geography, Gdańsk University, 4 Bażyńskiego St., Gdańsk 80-952, Poland.  
 Email: [kamil.nowinski@ug.edu.pl](mailto:kamil.nowinski@ug.edu.pl)

Żaneta Polkowska, Department of Analytical Chemistry, Faculty of Chemistry, Gdańsk University of Technology, 11 Gabriela Narutowicza St., Gdańsk 80-233, Poland.  
 Email: [zanpolko@pg.edu.pl](mailto:zanpolko@pg.edu.pl)

## Funding information

National Science Centre of Poland, Grant/Award Number: 2019/32/C/ST10/00483; Research Excellence Initiative of the University of Silesia in Katowice

## Abstract

Progressive climate change may have unpredictable consequences for the Arctic environment. Permafrost catchments off the west coast of Svalbard, described as “thin” and “warm,” are particularly sensitive to climate change. The interdisciplinary research on the hydrochemical response of surface and underground water functioning within a small permafrost catchment area focused on the determination of the impact of meteorological conditions (temperature ( $T$ ), precipitation ( $P$ )) on the mean daily discharge ( $Q$ ), and the lowering of the groundwater table ( $H$ ). We determined physical and chemical properties ( $pH$  and  $SEC$ ) and concentrations of major elements ( $Ca$ ,  $Mg$ ,  $Na$ ,  $K$ ) and 23 trace elements (i.a.  $Cd$ ,  $Cu$ ,  $Hg$ ,  $Pb$ ,  $Zn$ ) in 280 water samples. The results of the correlation matrix showed that an increase in the average air temperature in the summer of 2021 had a significant impact on the hydrochemistry of both types of waters operating in the catchment. In response to increase in  $T$ , the lowering of the  $H$  ( $0.52 < r < 0.66$ ) and a decrease in  $Q$  ( $-0.66 < r < -0.68$ ) were observed what in consequence also leads to changes in water chemistry. The principal component analysis (CA) indicates that chemical weathering and binding of elements to  $DOC$  are processes influencing water chemistry. Results of statistical analysis showed that the resultant of the hydrometeorological conditions that

prevailed in that season and the type of geological formations on which they were located had a significant impact on the water chemistry at individual measurement points. Significant differences in the concentrations of elements between points on the same geological formations were also found.

#### KEYWORDS

climate change, creek, element, metals, permafrost thawing, water pollution

## 1 | INTRODUCTION

In the 21st century, the Arctic is facing serious environmental transformations such as climate warming, leading to the intensification of glacier melting and thawing of permafrost (Biskaborn et al., 2019; Hanssen-Bauer et al., 2019; Szumińska et al., 2018; Wawrzyniak & Osuch, 2020). These phenomena promote the rapid retreat of glaciers and the expansion of Arctic permafrost areas. The changes are responsible for the acceleration of environmental processes occurring in the Arctic, from natural hydro- and geochemical reactions to the release of pollutants stored in glaciers and permafrost (AMAP, 2012; Dolnicki et al., 2013; Lehmann-Konera et al., 2018; Stachniak et al., 2022).

While permafrost accounts for up to 25% of the terrestrial part of the Earth, permafrost coastlines, mostly located in the Arctic, constitute approximately 34% of the world's coastlines (Christiansen et al., 2018, 2020; Lantuit et al., 2013). Research on mean temperatures of permafrost at a depth of 10–20 m in Svalbard shows that western coastal sites are warmer than the central part (between  $-2.5^{\circ}\text{C}$  and approximately  $-5^{\circ}\text{C}$ , respectively) (Hanssen-Bauer et al., 2019). Permafrost on the Svalbard west coast is therefore referred to as “warm” and “thin” (Kristensen, 2008) and is vulnerable to climate change (Christiansen et al., 2018). An increase in the thickness of the active layer results in an increase in infiltration of the ground (soil or rock) and changes in hydrological conditions related to the flow and storage of water. This consequently leads to alterations of the surface water level (Lehmann-Konera et al., 2018; Stachniak et al., 2022; White et al., 2007) and catchment geochemistry (Abbott et al., 2015; Carey, 2003; Larouche et al., 2015; Petrone et al., 2006).

The Svalbard Archipelago is a region of the Arctic that has been insufficiently investigated with respect to the chemical composition of groundwaters and surface waters in permafrost catchments. Studies on Svalbard's surface waters such as lakes, rivers, and streams are quite common for organic compound analysis (Kozak et al., 2017; Kwok et al., 2013; Lehmann-Konera et al., 2018, 2019, 2020; Polkowska et al., 2011) as well as ions and elemental composition (Kozak et al., 2015; Lehmann-Konera et al., 2021; Stachniak et al., 2016, 2019; Szumińska et al., 2018). Some studies in glacier-covered catchments of Svalbard also concern chemical composition of groundwaters in terms of major ions (Cooper et al., 2002; Dragon et al., 2015; Dragon & Marciniak, 2010; Olichwer et al., 2013; Wadham et al., 2007). However, there is a knowledge gap regarding the trace elements composition of the shallow groundwaters of permafrost catchments in Svalbard, as well as the impact of hydrometeorological conditions on changes in their levels.

This paper aims at providing a new insight into the hydrochemical variability of surface and subsurface water in a permafrost catchment in the coastal area of Bellsund and to define the effect of changing hydro-meteorological conditions on the element composition in particular parts of the catchment. The study covered the Rensdyrbekken (Reindeer Creek) catchment. An interdisciplinary team carried out hydrometeorological monitoring of mean daily water flow rate ( $Q$ ), as well as measurement of shallow groundwater levels ( $H$ ), average air temperature ( $T$ ), and precipitation magnitude ( $P$ ) in summer 2021. Furthermore, for a period of 30 days, 280 water samples were collected for chemical analyses. Chemical analyses included the determination of the following physico-chemical properties:  $pH$ , specific electrolytic conductivity ( $SEC$ ), dissolved organic carbon ( $DOC$ ), as well as major ( $Na$ ,  $Ca$ ,  $Mg$ ,  $K$ ) and trace elements ( $Ag$ ,  $Al$ ,  $As$ ,  $B$ ,  $Ba$ ,  $Be$ ,  $Bi$ ,  $Cd$ ,  $Co$ ,  $Cr$ ,  $Cu$ ,  $Fe$ ,  $Hg$ ,  $Li$ ,  $Mn$ ,  $Mo$ ,  $Ni$ ,  $Pb$ ,  $Sb$ ,  $Se$ ,  $Sr$ ,  $V$ , and  $Zn$ ) in all types of collected water samples. Moreover, photogrammetry and morphometry surveys were carried out to support the interpretation of the obtained results, permitting the determination of the catchment boundaries, elevation profile, and runoff lines.

## 2 | MATERIALS AND METHODS

The interdisciplinary research carried out within the framework of the research project included both photogrammetric and morphometric investigation of the Rensdyrbekken catchment, as well as meteorological observations, hydrological monitoring, and chemical analyses of various types of water functioning within the permafrost catchment in the High Arctic. This publication focuses on describing the spatial discrepancies in hydrochemical features of water functioning within a non-glaciated catchment. Therefore, all detailed information on research other than chemical analysis is included in Data S1.

### 2.1 | Study area and regional settings

The Svalbard Archipelago is in the zone of continuous permafrost (Dolnicki et al., 2013). Its thickness near the coast is less than 100 m and reaches more than 500 m in inland areas with high elevation (Dolnicki et al., 2013; Humlum et al., 2003; Kristensen, 2008). The thickness of the active layer at the west coast and in the central part of Spitsbergen is in a range of 100–200 cm (Hanssen-Bauer et al., 2019). Research on mean temperatures of permafrost at a depth of 10–20 m in Svalbard shows that western coastal sites are warmer than the central part (between  $-2.5^{\circ}\text{C}$  and approximately  $-5^{\circ}\text{C}$ ,

respectively) (Hanssen-Bauer et al., 2019). Permafrost on the Svalbard west coast is therefore referred to as “warm” and “thin” (Kristensen, 2008) and is vulnerable to climate change (Christiansen et al., 2018).

The High Arctic permafrost catchment of the Rensdyrbekken (Figure 1) drains an area of approximately 1.3 km<sup>2</sup> in the NW Part of the Wedel-Jarlsberg Land (Bellsund, Spitsbergen). The catchment is located on the tectonic units of the Calypsostranda Graben. The layer of active permafrost in the study area can reach a thickness of more than 202 cm (Marsz et al., 2013). The surface waters have snow-precipitation-permafrost alimentation regime (Harasimiuk & Gajek, 2013; Lehmann-Konera et al., 2018). The drainage system of the subsurface water is very well-developed due to the domination of brown soils with a light granulometric composition in the catchment area (Klimowicz et al., 2013).

## 2.2 | Hydrometeorological monitoring and sampling

Research regarding measurements of hydrometeorological conditions in the Rensdyrbekken catchment and the spatial distribution of elements in groundwaters and surface waters was conducted between June 23 and July 23, 2021 (Figure 2). A total of 124 surface water samples were collected during the period directly from the creek, 152 groundwater samples from piezometers.

Meteorological measurements were conducted in the central part of the catchment and covered air temperature ( $T$ ) and precipitation ( $P$ ) occurrence (CR at 38 m a.s.l.). Surface water sample collection and hydrological measurements of mean daily water discharge ( $Q$ ) in the Rensdyrbekken were conducted for 4 key cross-sections: a fragment

of the estuarine course of the river (RM at 13 m a.s.l.) morphologically constituting a watershed section; the middle course of the river together with its left-hand tributary (RMC; RLT—both at 20 m a.s.l.), where the terrain forms a scoured, flattened depression with a significant proportion of wetlands, and the source zone of the river (RS at 69 m a.s.l.), which is a highly elevated marine terraced area with a slight slope. Measurements of the groundwater table level ( $H$ ) and water sampling were also conducted in 6 piezometric boreholes. The distribution of these measurement points covered: the lower part of the Rensdyrbekken catchment, in the zones of elevated terrain on both sides of the watercourse (PZR\_6; PZR\_2—both at 27 m a.s.l.); the middle section of the catchment basin with a single point (PZR\_5 at 22 m a.s.l.) near the confluence of tributaries, and two points covering the higher parts of the middle part of the catchment (PZR\_3 at 29 m a.s.l.; PZR\_4 at 32 m a.s.l.) and the upper part of the catchment, which is an elevated marine terrace, with the piezometer on its left wing (PZR\_1 at 69 m a.s.l.).

## 2.3 | Data collection and sampling methods

Photogrammetric and morphometric surveys were used to prepare maps illustrating the morphometry of the catchment during the implementation of the field survey in the summer of 2021. The field materials were collected with use of eBee X fixed-wing drone equipped with a SensiFly Aeria X camera. Further, the data were subject to photogrammetric processing in the Agisurf Metashape Professional environment and imported to the WGS84/UTM zone33 system (more details in Data S1).

Flow conditions was measured in the RS, RMC, RM, and RLT section of the creek (Figure 2). Water stages were recorded 144 times

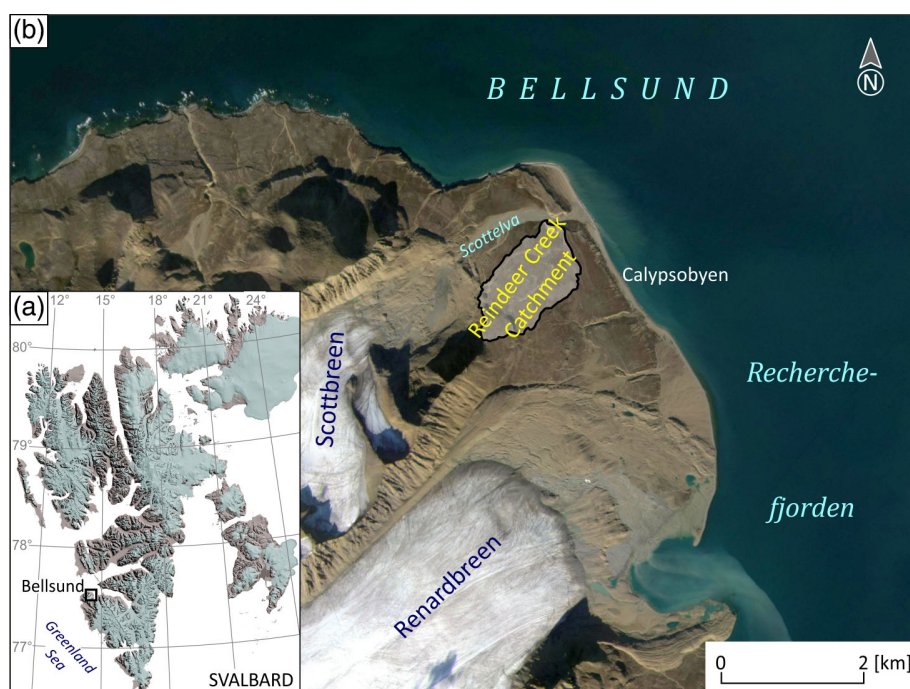
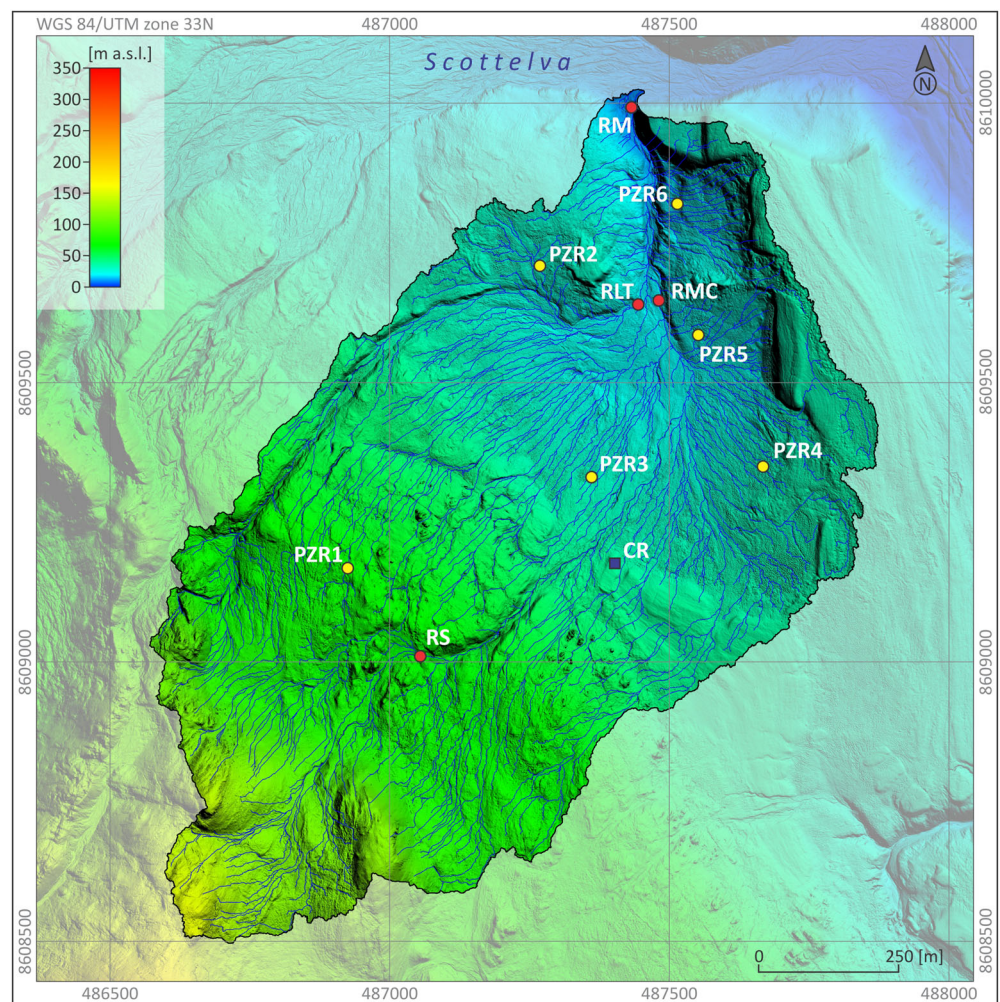


**FIGURE 1** Map of Svalbard (a) with location of the Rensdyrbekken catchment in the coastal area of Bellsund (b) (Background: Satellite image, 08/25/2020 – Planet Labs Inc.). [Colour figure can be viewed at [wileyonlinelibrary.com](http://wileyonlinelibrary.com)]



**FIGURE 2** Map of Rensdyrbekken catchment with points of hydrological measurements and sampling in surface water (red dots), groundwater (yellow dots), and meteorological measurements point (blue square) (Background: flow network generated based on DEM). [Colour figure can be viewed at [wileyonlinelibrary.com](https://onlinelibrary.wiley.com/doi/10.1002/ldr.5028)]



per day with TD-Diver meter (Eijkelkamp), with a measurement accuracy of  $\pm 0.5$  cm. The flow velocity was measured by a HEGA I (Biomix, Poland) current meter, with a range of flow velocity measurements of  $0.02$ – $3.00$   $\text{m s}^{-1}$  and  $0.2$ – $2.4$   $\text{m s}^{-1}$  (and an accuracy of  $\pm 0.25$   $\text{m s}^{-1}$ ), respectively. More details and calculations of mean daily discharge are given in Data S1. Measurements of the position of the groundwater table were conducted in the installed piezometers PZR\_1–6 (Figure 2). Registration of water levels was carried out manually using a hydrogeological whistle at a frequency of once a day.

Air temperature was measured every 10 min with an automatic temperature datalogger HOBO U12 Stainless Temp Logger. While precipitation was collected with Pronamic Rain-O-Matic Professional rain gauge (CR in Figure 2) with  $200$   $\text{cm}^2$  inlet surface area, mounted on a stand.

The water samples were collected into  $0.25$ – $0.5$  L chemically clean plastic bottles made of high-density polyethylene (HDPE). The personnel were equipped with polyethylene gloves to prevent contamination of samples. Surface water samples were collected manually to bottles previously triple rinsed with the sampled water. Groundwater sampling employed a peristaltic pump (Eijkelkamp Soil & Water company). The composition stability and representativeness of water samples for organic analysis were ensured by their filtering

through glass microfiber  $47$  mm GF/C Whatman filters. For inorganic analysis, the samples were filtered through a  $0.45$   $\mu\text{m}$  PTFE filter to  $50$  mL plastic vials and subject to acidification by  $\text{HNO}_3$  (ultrapure). The samples were stored in dark conditions at a temperature of approximately  $4^\circ\text{C}$  for transportation. To mitigate the impact of the procedure and sample containers, a blank sample was used as a control.

## 2.4 | Chemical analysis

In situ measurements of physicochemical properties of groundwater and surface water employed a multi-parameter YSI Pro1030 pH/conductivity meter. The analysis of dissolved organic carbon (DOC) and elements (Ag, Al, As, B, Ba, Be, Bi, Ca, Cd, Co, Cr, Cu, Fe, Hg, K, Li, Mg, Mn, Mo, Na, Ni, Pb, Sb, Se, Sr, V, and Zn) was conducted after the delivery of samples to the laboratory in Poland. Both in the field and in Poland, deionized water of Mili-Q type (Mili-Q® Ultrapure Water Purification Systems, Millipore®) was used during the analytical procedures. DOC was determined by catalytic combustion (oxidation) by means of an NDIR detector (Total Organic Carbon Analyzer TOC-VCSH/CSN, SHIMADZU, Japan, Potassium Hydrogen Phthalate

standard). The elements analysis was performed by means of Inductively Coupled Plasma Mass Spectrometry (ICP-MS 2030 Shimadzu, Japan). The inorganic analysis conditions were as follows: Collision Cell Technology, plasma gas flow Ar: 8 L/min, collision cell gas flow He: 6 mL/min. The quality of the analysis was ensured due to use of standards (CRM-IV multi-element standard, Merck, USA); single standards: As, Sb, Se, Mo, and V (Sigma-Aldrich, USA); internal standard of Sc, Rh, Tb, and Ge in 1% HNO<sub>3</sub> solution (Merck, USA), and the application of certified reference materials (CRM ERM-CA713 (sample 125)) of trace elements in wastewater (IRMM—Institute for Reference Materials and Measurements). Details concerning validation parameters such as limit of detection (LOD) and limit of quantification (LOQ) are given in (Table S1).

## 2.5 | Statistical analysis

The statistical analysis of data employed a Mann–Whitney U test, matrix correlation analysis, and cluster analysis (CA). All statistics were performed for two-tailed  $\alpha = 0.05$ , using STATISTICA 13.3 (TIBCO®, StatSoft Inc., Tulsa, OK, USA) software and/or Python programming language. Details of the computational methods used to analyze the data can be found in Data S1 as well as the results of Mann–Whitney U test (Tables S3 and S4).

## 3 | RESULTS

### 3.1 | Discrepancies in chemical water properties

The results of hydrometeorological measurements and values of chemical analysis results are provided in Table 1, and Figures S2–S4 and Table S2. As shown in Table 1 mean daily air temperature varied significantly between 2.09 and 7.44°C. Only 6 daily total precipitation was noted during that time (Figure S2).

The discharge values varied from 0.750 up to 145 L/s between the spring and mouth of the creek, respectively (Table 1, Figure S3). While the fluctuations of water table varied from 0 to 82 cm below ground level (b.g.l) between PZR\_1 and PZR\_2, respectively (Table 1, Figure S4). Statistically significant differences of hydrological conditions were observed between the Rensdyrbekken spring (RS), main course (RMC), mouth (RM), and left tributary (RLT) sections (Tables S2 and S3). In the case of groundwater level, the discrepancies were only significant between PZR\_2 and PZR\_3–6 (Tables S2 and S3, Figure 3).

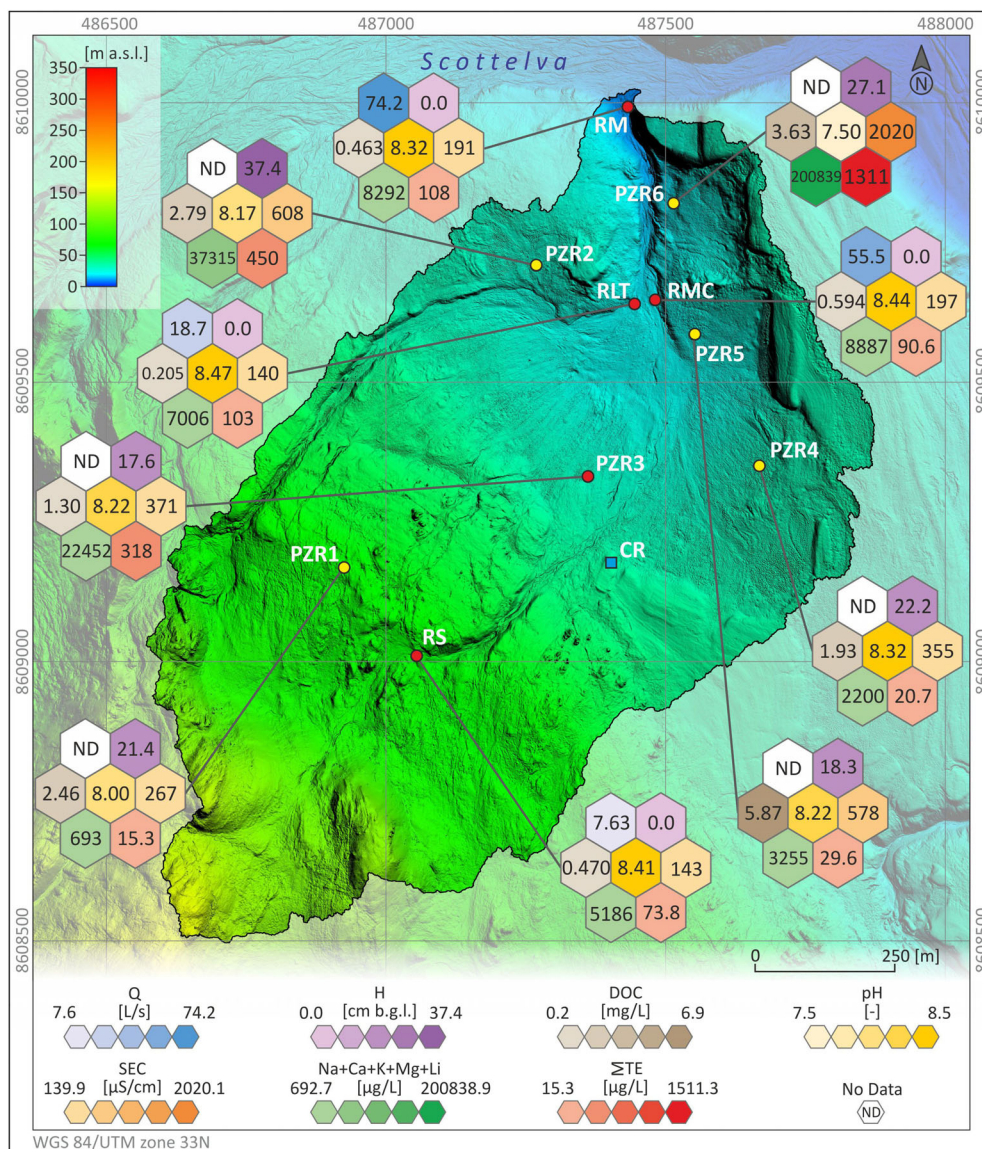
In the case of physicochemical parameters in the catchment water pH oscillated between 7.18 in groundwater and 8.86 in surface water (Table 1). The highest mean values of water pH were observed in RLT and the lowest in PZR\_6 (Figure 3). Similarities in water pH were noted for RS with RMC; RMC with RLT; PZR\_2 with PZR\_3 and 5; PZR\_3 with PZR 4 and 5; and PZR\_4 with PZR\_5 (Tables S2 and S3). The levels of SEC varied in surface water and groundwater from 71.5–250  $\mu\text{S}/\text{cm}$  to 167–2,708  $\mu\text{S}/\text{cm}$ , respectively (Table 1). The lowest mean value of SEC was characteristic of RLT and the highest of

**TABLE 1** Data of results of hydrometeorological monitoring (Q, H, P, T), and ranges of values of determined physicochemical parameters (pH, SEC), sum parameter (DOC), as well as elements in water samples collected from the studied catchment.

Determined parameters/ analytes	Rensdyrbekken	
	Surface water	Groundwater
	RS, RMC, RLT, RM	PZR_1–6
	Min–Max	
Meteorological measurements		
T [°C]	2.09–7.44	
P [mm]	0–6.55	
Hydrological measurements		
Q [L/s]	0.750–145	n.d.
H [cm b.g.l]	n.d.	0–82
Physicochemical measurements		
pH [–]	7.93–8.86	7.18–8.62
SEC [ $\mu\text{S}/\text{cm}$ ]	71.5–250	167–2,708
Sum parameter		
DOC [mg/L]	0.104–1.07	0.597–10.8
Elements [ $\mu\text{g}/\text{L}$ ]		
Ag	0.004–0.423	<LOD – 1.97
Al	1.69–66.9	<LOD – 124
As	0.045–0.351	0.003–2.77
B	0.687–10.7	<LOD – 226
Ba	0.942–26.7	0.719–1,050
Be	0.108–0.316	<LOD – 2.58
Bi	<LOD	<LOD – 0.405
Ca	224–1,120	78.4–17,300
Cd	0.004–0.851	0.010–5.97
Co	0.007–0.303	<LOD – 1.12
Cr	0.057–20.7	<LOD – 6.75
Cu	0.056–9.52	<LOD – 208
Fe	4.35–57.5	<LOD – 363
Hg	<LOD	<LOD – 0.051
K	60.0–565	<LOD – 13,700
Li	0.095–3.69	<LOD – 310
Mg	1,810–9,420	194–318,000
Mn	0.143–3.93	<LOD – 326
Mo	0.054–45.7	0.030–11.1
Na	57.2–431	35.5–7,870
Ni	0.067–1.28	<LOD – 6.09
Pb	0.144–14.6	0.016–191
Sb	0.019–0.424	0.014–7.76
Se	0.051–0.278	0.023–0.860
Sr	12.5–74.7	3.43–1,790
V	0.006–0.382	0.001–0.512
Zn	0.483–14.6	<LOD – 1,100



**FIGURE 3** Map of the permafrost catchment area with the average values of the results of hydrology and physicochemical parameters at the measurement points of surface water (RSM RMC, RLT, RM; red dots) and shallow groundwater (PZR\_1–6; yellow dots). [Colour figure can be viewed at [wileyonlinelibrary.com](https://onlinelibrary.wiley.com/doi/10.1002/ldr.5028)]



PZR\_6 (Figure 3). Statistical differences were observed for SEC between all groundwater sampling sites (Table S3) and for RS with RMC and RM, as well as RLT with RMC and RM (Table S2). Dissolved organic carbon showed significant differences between sites (Tables S2 and S3). The concentrations of DOC in RS, RMC, RLT, and RM did not exceed 1.07 mg/L (Table 1), with similarities in levels between sites RS and RM (Table S2) which mean values of approximately 470 mg/L (Figure 3). For surface water sites, RMC showed the highest mean value of DOC (0.594 mg/L) and RLT the lowest one (0.205 mg/L) (Figure 3). DOC in groundwater samples varied from 0.597 to 10.8 mg/L, with significant differences between sites. The lowest DOC level (0.104 mg/L) was observed at site RLT and the highest one (10.8 mg/L) at both PZR\_5 and PZR\_6 (Table 1, Table S2).

The elements composition between sites differs significantly in most cases (Tables S2 and S3). It should be emphasized that Bi and Hg were below limit of detection (<LOD) in all surface water samples. At groundwater study sites, Bi was <LOD at PZR\_2 and PZR\_3, and Hg was <LOD at PZR\_1–5 but occurred at PZR\_6. Moreover, study sites

PZR\_1, 4, and 5 were mostly characterized by composition of elements lower than that of any other study site (Figure 3). At these study sites, <LOD concerned Ag, Al, B, Be, Co, Cr, Cu, Mn, Ni, Zn, and occasionally Fe, K, and Li (Table 1). Surface water composition showed similarities of RS and RMC in concentration of Ba, Fe, Mn, Mo, Ni, Se, and V. For RS and RLT, comparable levels occurred in case of Al, Ba, Ca, Fe, and V. RS and RM show corresponding concentrations of Al, As, Fe, Pb, and Se. Only some similarities in levels of Se and V are recorded between the main course of the creek and its left tributary. Although RMC is the main course of the creek, the left tributary of the Rensdyrbekken shows more similarities in elements composition with the mouth section (RM). In the first case (RMC/RM), it concerns only Ag, Mg, and Sr, and in the second case (RLT/RM) Al, B, Ba, Be, Cd, Cr, Cu, Fe, Li, Mo, Pb, and Zn (Table S2). In groundwater samples, similarities in elemental composition were observed between PZR\_1, 4, and 5 for elements such as Al, Ba, Cd, Fe, Li, Mn, Pb, Sb, Sr, V, and Zn. The mean value of major elements at these sites varied between 693 and 3,255 µg/L, and for sum of trace elements ( $\Sigma_{TE}$ ) between 15.3

and 29.6  $\mu\text{g/L}$  (Figure 3). PZR\_2 and PZR\_3 showed similar concentrations of As, Be, Cd, Fe, Pb, Se, and Zn. These sites were also characterized by higher mean values of major elements (37,314  $\mu\text{g/L}$  and 22,452  $\mu\text{g/L}$ , respectively) and  $\Sigma_{\text{TE}}$  (450  $\mu\text{g/L}$  and 318  $\mu\text{g/L}$ , respectively) than in the case of PZR\_1, 4, and 5 (Figure 3). Comparable levels of Zn were also observed between PZR\_6 with PZR\_2 and 3. PZR\_6 stood out from all other study sites with the highest mean values of major and  $\Sigma_{\text{TE}}$  (200,839  $\mu\text{g/L}$  and 1,311  $\mu\text{g/L}$ , respectively) (Figure 3). Moreover, PZR\_3 and 6 showed similarities in concentrations of Mo and Sb, while PZR\_4 and 5 had comparable levels of Cd, Mn, Mo, Pb, and Se (Table 1).

The results of cluster analysis (CA) (Figure 4. RS, RMC, RM, RLT) permitted the designation of 3 major clusters in the surface water of the Rensdyrbekken catchment at sites RS, RLT, and RMC, despite the

differences in elements composition. In the case of RM, elements are grouped in only 2 major clusters. Different cluster analysis groups can be distinguished by their relationship to pH, SEC, and DOC. In the source section of the stream, elements such as Mo, Cu, Ag, Cr, Fe, Ni, Pb, Zn, Al, and Mn form the first group RS\_C1, showing correlations with pH, SEC, and DOC. No such correlations were observed at the other sites. At site RMC, the first cluster RMC\_C1, including B, K, Na, Li, Mg, Ca, and Sr, shows links to pH and SEC. Only the third cluster RMC\_C3 represented by Ag, Ba, As, Se, Al, V, Be, and Cr shows an association with DOC. Waters from the left tributary of the stream showed some similarity in grouping of elements in RLT\_C1 (Mo, B, Li, K, Sr, Ca, Mg, Be) with RMC\_C1, and their association with pH and SEC. A similarity was also observed in the grouping of elements in RLT\_C2 (Se, Na, Ag, Ba, As) with RMC\_C3 and their association with

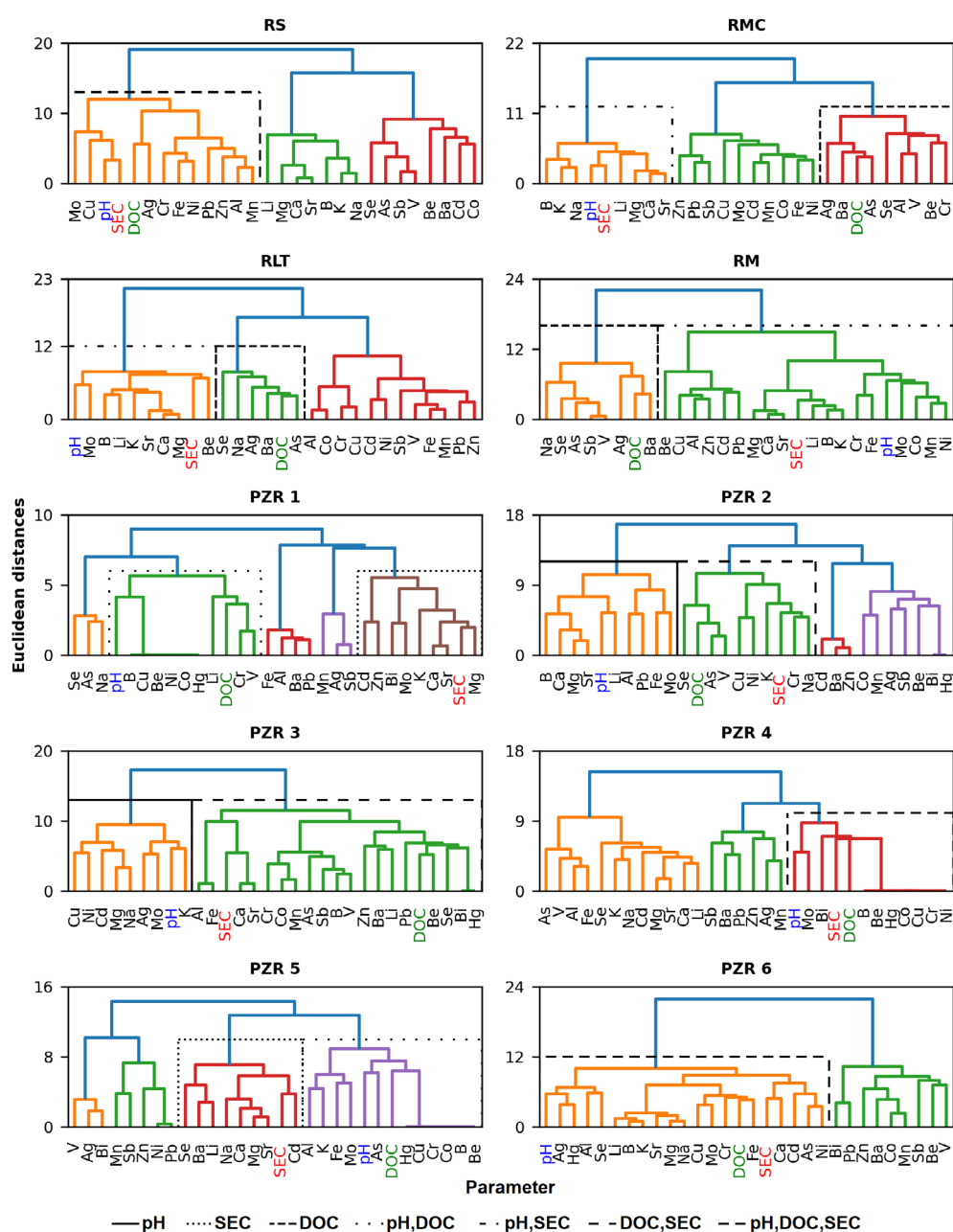


**FIGURE 4** Hierarchical dendrograms resulting from cluster analysis of sum parameter and physicochemical indices in the surface water (RS, RMC, RM, RLT) and groundwater (PZR\_1–6) of the Rensdyrbekken. Clustering was performed on standardized values, with Ward's method, using squared Euclidean distance. Major clusters characterized by association with pH, SEC, or DOC were marked with a line described in the legend of the figure. [Colour figure can be viewed at [wileyonlinelibrary.com](https://onlinelibrary.wiley.com)]

DOC. Like in RS\_C2 and C3, elements grouped in RMC\_C2 and RLT\_C3 show no association with *pH*, *SEC*, or *DOC*. Against the background of these correlations, the estuary section of the stream is distinguished by the occurrence of only two groups of elements RM\_C1 where elements *Na*, *Se*, *As*, *Sb*, *V*, *Ag*, and *Ba* show correlations with *DOC*. Meanwhile, in RM\_C2, elements such as *Be*, *Cu*, *Al*, *Zn*, *Cd*, *Pb*, *Mg*, *Ca*, *Sr*, *Li*, *B*, *K*, *Cr*, *Fe*, *Mo*, *Co*, *Mn*, and *Ni* were characterized by an association with *pH* and *SEC*.

Cluster analysis of the groundwater chemistry (Figure 4. PZR\_1–6) shows very high variability between the sites. Water samples from PZR\_1 had the most numerous clusters (PZR\_1-C1 to C5). PZR\_2–6 was characterized by a division of elemental composition into 2–4 main clusters. A relation to *pH* was determined for elements belonging to clusters PZR\_2-C1 (*B*, *Ca*, *Mg*, *Sr*, *Li*, *Al*, *Pb*, *Fe*, *Mo*) and PZR\_3-C1 (*Cu*, *Ni*, *Cd*, *Mg*, *Na*, *Ag*, *Mo*, *K*). Elements whose presence was associated with *SEC* were included in clusters PZR\_1-C5 (*Cd*, *Zn*, *Bi*, *Mo*, *K*, *Ca*, *Sr*, *Mg*) and PZR\_5-C3 (*Se*, *Ba*, *Li*, *Na*, *Ca*, *Mg*, *Sr*, *Cd*). Elements in clusters PZR\_1-C2 (*B*, *Cu*, *Be*, *Ni*, *Co*, *Hg*, *Li*, *Cr*, *V*) and PZR\_5-C4 (*Al*, *K*, *Fe*, *Mo*, *As*, *Hg*, *Cu*, *Cr*, *Co*, *B*, *Be*) showed association with *pH* and *DOC*. A relation to both *SEC* and *DOC* were noted for elements belonging to clusters PZR\_2-C2 (*Se*, *As*, *V*, *Cu*, *Ni*, *K*, *Cr*, *Na*) and PZR\_3-C2 (*Al*, *Fe*, *Ca*, *Sr*, *Cr*, *Co*, *Mn*, *As*, *Sb*, *B*, *V*, *Zn*, *Ba*, *Li*, *Pb*, *Be*, *Se*, *Bi*, *Hg*). Elements whose presence was associated with *pH*, *SEC* and *DOC* were included in clusters PZR\_4-C3 (*Mo*, *Bi*, *B*, *Be*, *Hg*, *Co*, *Cu*, *Cr*, *Ni*) and PZR\_6-C2 (*Ag*, *Hg*, *Al*, *Se*, *Li*, *B*, *K*, *Sr*, *Mg*, *Na*, *Cu*, *Mo*, *Cr*, *Fe*, *Ca*, *Cd*, *As*, *Ni*). Elements in clusters PZR\_1 (C1, C3 and C4), PZR\_2 (C3 and C4), PZR\_4 (C1 and C2), PZR\_5 (C1 and C2), and PZR\_6 (C2) showed no association with *pH*, *SEC*, and *DOC*.

### 3.2 | Relationship between meteorological conditions and catchment hydrochemistry

Table 2 presents results of a matrix correlation analysis between the meteorological conditions and hydrochemistry of the Rensdyrbekken catchment. A statistically significant negative correlation between *Q* and *T* ( $-0.66 < r < -0.68$ ), *pH* ( $-0.63 < r < -0.85$ ), and *SEC* ( $-0.79 < r < -0.91$ ) was recorded in all sections of the analyzed surface water except for RLT. On the contrary, a significant positive correlation was observed between *T* and water *pH* ( $0.36 < r < 0.61$ ) at all measurement sites and *SEC* along the course of the main watercourse from RS ( $r = 0.42$ ) through RMC ( $r = 0.53$ ) and RM ( $r = 0.49$ ). *DOC* showed no correlation with hydrochemistry in the RS section. By contrast, statistically significant positive correlations of *DOC* with *Q* were observed in the RMC ( $r = 0.75$ ) and RM ( $r = 0.84$ ) sections, and negative correlations with *T* in the RMC ( $r = -0.62$ ), RLT ( $r = -0.64$ ), and RM ( $r = -0.48$ ) sections.

Regarding the effect of hydrological factors on the element composition of surface water, a significantly positive correlation was determined in the RS section for *Q* with *As*, *Ba*, *Na*, *Sb*, *Se*, and *V*, in RMC only with *Ag*, *As*, and *Ba*, and in RM with *Ag*, *As*, *Ba*, *Sb*, *Se*, and *V*. A significant negative correlation was recorded for *Q* with *Cu*, *Mg*, and *Mo* in the RS section, with *B*, *Ca*, *Co*, *Fe*, *K*, *Li*, *Mg*, *Mo*, *Na*, *Ni*, and *Sr* in the RMC section, with *B*, *Ca*, *K*, and *Mg* in the left tributary of the stream, and with *B*, *Ca*, *Co*, *Cr*, *Fe*, *K*, *Li*, *Mg*, *Mn*, *Mo*, *Ni*, and *Sr*.

Meteorological conditions prevailing in the catchment area such as mean air temperature (*T*) showed a significantly positive correlation with *Fe*, *Mg*, *Mn*, *Mo*, *Ni*, and *Zn* in RS, with *B*, *Ca*, *Cd*, *Co*, *Cu*, *Fe*, *K*, *Li*, *Mg*, *Mn*, *Mo*, *Ni*, *Sr*, and *Zn* in the main stream, with *B*, *Ca*, and *Mo* in the left tributary, and with *B*, *Ca*, *Co*, *Cr*, *Fe*, *K*, *Li*, *Mg*, *Mn*, *Ni*, *Sr*, and *Zn* in the RM section. A significantly negative correlation of *T* with *As* was recorded in all surface water monitoring points, with *Ba* in RMC and RLT, and with *Sb*, *Se*, and *V* in the RS and RM sections. The occurrence of rainfall (*P*) showed no significant effect on the hydrochemistry of the stream, except for the correlation with *Ba* ( $r = 0.41$ ) in the RM section.

In the case of groundwater (Table 3), on the contrary, the hydrological variable (*H*) showed a statistically significant positive correlation with *T* ( $0.52 < r < 0.66$ ) in all measurement points, with water *pH* at PZR\_2, 3, 4, and 6 ( $0.52 < r < 0.64$ ), and with *SEC* at PZR\_5 and 6 ( $r = 0.80$  and  $r = 0.37$ , respectively). Moreover, there was also a statistically significant positive correlation between *T* and water *pH* in PZR\_2, 3, 4, and 6. Rainfall (*P*) showed a statistically significant correlation with water *pH* ( $r = 0.90$ ) only in PZR\_1.

At monitoring site PZR\_1, the hydrometeorological factors in the catchment showed a statistically significant negative correlation only with *Mn* ( $r = -0.75$ ). In the remaining monitoring points, the correlations between the variation of hydrometeorological conditions of the catchment and the elements were much more diverse. Moreover, the significant positive correlation between *H* and *T* in groundwater implies their further relationship with the presence of elements in different parts of the catchment. In PZR\_2, these factors correlate negatively with *Ag*, *As*, *Se*, and *V*, and positively with *Cd*, *Cr*, *Li*, *Mg*, *Na*, and *Sr*. In PZR\_3, positive correlations of *H* and *T* are observed with *Ag*, *Cd*, *Cu*, *Mg*, *Mo*, and *Na*, and negatively with *As*, *B*, *Be*, *Ca*, *Co*, *Cr*, *Mn*, *Sb*, *Sr*, *V*, and *Zn*. A significant positive correlation between *H* and *T* in groundwater projects their further relationship to the presence of the elements in different parts of the catchment. In PZR\_2, these factors correlate negatively with *Ag*, *As*, *Se*, and *V*, and positively with *Cd*, *Cr*, *Li*, *Mg*, *Na*, and *Sr*. In PZR\_3, positive correlations of *H* and *T* are observed with *Ag*, *Cd*, *Cu*, *Mg*, *Mo*, *Na*, and *Na*, and negative with *As*, *B*, *Be*, *Ca*, *Co*, *Cr*, *Mn*, *Sb*, *Sr*, *V*, and *Zn*. In PZR\_4, *H* significantly negatively correlates only with *Ba*, and *T* with *Ag*. For both *H* and *T*, there were significant positive correlations with *Al*, *As*, *Ca*, *Cd*, *Fe*, *K*, *Li*, *Mg*, *Na*, *Se*, *Sr*, and *V*. Like in PZR\_4, in PZR\_5 *H* and *T* significantly positively correlated with *Al*, *Ca*, *Cd*, *K*, *Li*, *Mg*, *Na*, and *Sr*, while *T* was significantly negatively correlated only with *Ag* and *Bi*. Like in PZR\_3, in PZR\_6 significant negative correlations were also recorded between *H* and *T* with *Ba*, *Be*, *Co*, *Mn*, and *Zn*. Monitoring point PZR\_6 showed the highest number of significant positive correlations between *H* and *T* and elements present at the study site such as *Ag*, *As*, *B*, *Ca*, *Cd*, *Cr*, *Cu*, *Fe*, *Hg*, *K*, *Li*, *Mg*, *Mo*, *Na*, *Ni*, and *Sr*.

## 4 | DISCUSSION

### 4.1 | Impact of meteorological conditions

The key factors shaping water chemistry on Svalbard include dry and wet deposition of contaminants and rock-water interactions (Cooper



**TABLE 2** Matrix correlation analysis results of meteorological data and results of physicochemical parameters, and elements in surface water samples.

RS	T	P	pH	SEC	DOC	Ag	Al	As	B	Ba	Be	Ca	Cd	Co	Cr	Cu	Fe	K	Li	Mg	Mn	Mo	Na	Ni	Pb	Sb	Se	Sr	V	Zn	
Q	-0.66	0.19	-0.85	-0.85	0.29	-0.12	0.15	0.84	0.02	0.73	0.28	-0.05	0.26	0.22	-0.35	-0.43	-0.20	0.29	0.02	-0.45	-0.05	-0.52	0.36	-0.33	0.07	0.62	0.49	-0.15	0.47	-0.13	
T	0.02	0.48	0.42	0.00	0.30	0.26	-0.68	0.09	-0.33	-0.25	0.11	-0.05	0.04	0.35	0.28	0.37	-0.20	-0.14	0.37	0.36	0.42	-0.33	0.41	0.13	-0.50	-0.45	0.17	-0.46	0.42		
P	-0.14	-0.33	0.03	-0.20	0.02	0.12	-0.13	0.07	-0.19	-0.10	-0.08	-0.15	-0.19	-0.14	-0.05	-0.07	0.10	-0.17	-0.08	-0.17	-0.10	-0.11	0.03	0.02	0.00	0.00	-0.11	-0.06	-0.06		
RMC	T	P	pH	SEC	DOC	Ag	Al	As	B <td>Ba</td> <td>Be</td> <td>Ca</td> <td>Cd</td> <td>Co</td> <td>Cr</td> <td>Cu</td> <td>Fe</td> <td>K</td> <td>Li</td> <td>Mg</td> <td>Mn</td> <td>Mo <td>Na</td> <td>Ni</td> <td>Pb</td> <td>Sb</td> <td>Se</td> <td>Sr</td> <td>V</td> <td>Zn</td> </td>	Ba	Be	Ca	Cd	Co	Cr	Cu	Fe	K	Li	Mg	Mn	Mo <td>Na</td> <td>Ni</td> <td>Pb</td> <td>Sb</td> <td>Se</td> <td>Sr</td> <td>V</td> <td>Zn</td>	Na	Ni	Pb	Sb	Se	Sr	V	Zn	
Q	-0.68	0.26	-0.85	-0.79	0.75	0.63	0.12	0.63	-0.76	0.75	0.02	-0.78	-0.35	-0.59	-0.10	-0.25	-0.50	-0.62	-0.72	-0.90	-0.28	-0.79	-0.63	-0.44	-0.01	-0.23	-0.11	-0.75	-0.13	-0.24	
T	0.02	0.56	0.53	-0.62	-0.35	-0.01	-0.42	0.55	-0.59	-0.03	0.48	0.47	0.56	0.10	0.42	0.55	0.40	0.47	0.56	0.44	0.67	0.26	0.46	0.21	0.33	0.11	0.50	0.15	0.36		
P	-0.16	-0.07	-0.11	0.05	-0.07	-0.06	-0.23	0.03	-0.08	-0.20	-0.07	-0.30	-0.07	-0.30	-0.15	-0.13	-0.20	-0.32	-0.17	-0.20	-0.07	-0.14	-0.29	-0.18	0.04	-0.22	0.21	-0.15	-0.31	-0.09	
RM	T	P	pH	SEC	DOC	Ag	Al	As	B <td>Ba</td> <td>Be</td> <td>Ca</td> <td>Cd</td> <td>Co</td> <td>Cr</td> <td>Cu</td> <td>Fe</td> <td>K</td> <td>Li</td> <td>Mg</td> <td>Mn</td> <td>Mo <td>Na</td> <td>Ni</td> <td>Pb</td> <td>Sb</td> <td>Se</td> <td>Sr</td> <td>V</td> <td>Zn</td> </td>	Ba	Be	Ca	Cd	Co	Cr	Cu	Fe	K	Li	Mg	Mn	Mo <td>Na</td> <td>Ni</td> <td>Pb</td> <td>Sb</td> <td>Se</td> <td>Sr</td> <td>V</td> <td>Zn</td>	Na	Ni	Pb	Sb	Se	Sr	V	Zn	
Q	-0.67	0.28	-0.63	-0.91	0.84	0.37	-0.04	0.73	-0.80	0.73	-0.10	-0.62	0.05	-0.61	-0.43	-0.35	-0.62	-0.76	-0.82	-0.77	-0.84	-0.51	-0.06	-0.88	0.13	0.50	0.36	-0.68	0.47	-0.37	
T	0.02	0.36	0.49	-0.48	-0.32	0.03	-0.62	0.58	-0.33	-0.01	0.39	0.00	0.43	0.46	0.18	0.50	0.48	0.51	0.51	0.61	0.61	0.18	-0.17	0.57	-0.15	-0.49	-0.40	0.43	-0.46	0.44	
P	-0.10	-0.23	0.21	-0.07	0.24	0.03	-0.18	0.41	-0.01	-0.12	0.35	-0.23	-0.01	0.02	-0.03	-0.20	-0.21	-0.13	-0.16	-0.16	-0.16	-0.13	-0.20	0.26	0.26	-0.05	-0.06	-0.15	-0.05	0.15	
RLT	T	P	pH	SEC	DOC	Ag	Al	As	B <td>Ba</td> <td>Be</td> <td>Ca</td> <td>Cd</td> <td>Co</td> <td>Cr</td> <td>Cu</td> <td>Fe</td> <td>K</td> <td>Li</td> <td>Mg</td> <td>Mn</td> <td>Mo <td>Na</td> <td>Ni</td> <td>Pb</td> <td>Sb</td> <td>Se</td> <td>Sr</td> <td>V</td> <td>Zn</td> </td>	Ba	Be	Ca	Cd	Co	Cr	Cu	Fe	K	Li	Mg	Mn	Mo <td>Na</td> <td>Ni</td> <td>Pb</td> <td>Sb</td> <td>Se</td> <td>Sr</td> <td>V</td> <td>Zn</td>	Na	Ni	Pb	Sb	Se	Sr	V	Zn	
Q	-0.25	0.30	-0.21	-0.30	0.24	0.35	0.13	0.15	-0.38	0.14	-0.25	-0.55	-0.01	0.04	-0.04	0.05	0.01	-0.55	-0.27	-0.55	0.05	0.02	-0.01	-0.03	0.22	-0.06	-0.07	-0.56	0.15	0.08	
T	0.02	0.61	0.26	-0.64	-0.17	-0.10	-0.49	0.45	-0.42	0.18	0.36	0.05	0.02	0.04	-0.09	0.23	0.06	0.33	0.33	0.33	0.18	0.36	0.18	0.36	0.21	0.04	0.15	-0.21	0.35	0.04	0.21
P	-0.15	-0.14	0.15	0.21	-0.11	0.06	-0.31	0.14	0.21	-0.18	-0.07	-0.14	-0.10	-0.14	-0.08	-0.17	-0.21	-0.28	-0.28	-0.18	-0.16	-0.11	-0.09	-0.16	-0.12	-0.12	-0.06	-0.13	-0.14	-0.11	

Note: Statistical significances ( $\alpha < 0.05$ ) were marked in bold and highlighted in grey.

**TABLE 3** Matrix correlation analysis results of meteorological data and results of physicochemical parameters, and elements in groundwater samples.

PZR		P	pH	SEC	DOC	Ag	Al	As	B	Ba	Be	Bi	Ca	Cd	Co	Cr	Cu	Fe	Hg	K	Li	Mg	Mn	Mo	Na	Ni	Pb	Sb	Se	Sr	V	Zn	
1	H	0.66	0.25	0.33	0.05	0.16	-0.39	0.39	0.14	nd	0.21	nd	0.16	0.02	-0.14	nd	0.00	nd	0.08	nd	0.26	0.42	0.32	-0.75	0.32	0.26	nd	0.40	-0.33	-0.17	0.13	-0.06	-0.17
	T	0.33	0.30	0.21	-0.23	0.17	0.07	0.14	nd	0.01	nd	-0.32	0.04	-0.39	nd	-0.32	nd	-0.06	nd	0.51	0.02	0.28	-0.37	0.11	0.28	nd	0.16	0.23	-0.02	0.19	-0.51	-0.10	
	P	0.90	-0.15	-0.08	-0.13	-0.13	-0.02	nd	-0.08	nd	-0.08	nd	-0.16	-0.13	-0.43	nd	-0.13	nd	-0.23	nd	0.41	-0.27	0.12	-0.29	0.26	-0.03	nd	0.14	-0.16	0.18	-0.02	-0.13	-0.24
2	H	0.52	-0.05	0.16	-0.31	-0.57	0.08	-0.40	0.03	0.35	-0.02	nd	0.15	0.51	-0.25	0.47	0.13	0.31	nd	0.24	0.64	0.60	-0.05	0.08	0.36	0.16	0.23	-0.29	-0.54	0.38	-0.43	0.29	
	T	0.10	0.41	0.24	-0.31	-0.39	0.06	-0.34	0.21	0.04	-0.08	nd	0.33	0.09	-0.21	0.05	0.06	0.08	nd	0.11	0.49	0.60	0.29	-0.06	0.22	-0.04	-0.01	-0.31	-0.30	0.53	-0.31	0.00	
	P	0.06	0.19	-0.02	-0.03	0.01	0.10	-0.12	-0.05	-0.02	nd	-0.02	-0.09	-0.10	-0.09	-0.08	-0.21	nd	-0.12	0.18	0.03	0.03	-0.09	-0.13	0.12	0.03	-0.06	-0.04	-0.01	0.08	0.11	0.03	
3	H	0.53	-0.19	0.61	-0.17	-0.50	0.44	-0.24	-0.47	-0.50	-0.29	-0.41	nd	-0.41	0.47	-0.21	-0.40	0.61	-0.28	nd	0.31	-0.04	0.58	-0.14	0.46	0.55	0.19	-0.29	-0.60	-0.13	-0.38	-0.56	-0.54
	T	0.11	0.48	-0.31	-0.30	0.48	-0.05	-0.55	-0.57	-0.08	-0.43	nd	-0.44	0.17	-0.45	-0.51	0.23	-0.04	nd	0.13	-0.17	0.32	-0.44	0.17	0.37	0.17	-0.09	-0.54	-0.35	-0.45	-0.59	-0.25	
	P	0.07	-0.14	-0.20	-0.09	-0.06	-0.10	0.01	0.28	0.19	nd	-0.01	0.00	-0.11	-0.04	-0.10	-0.05	nd	-0.37	0.04	-0.01	-0.09	-0.09	-0.22	0.10	-0.15	-0.02	0.06	0.05	-0.06	-0.02	0.46	
4	H	0.58	-0.11	0.55	0.19	-0.12	-0.36	0.42	0.43	nd	-0.43	nd	-0.30	0.58	0.66	nd	nd	0.65	nd	0.55	0.70	0.87	-0.15	0.12	0.61	nd	-0.26	-0.15	0.59	0.89	0.58	-0.36	
	T	0.12	0.46	0.46	-0.11	-0.61	0.28	0.18	nd	-0.28	nd	-0.36	0.45	0.15	nd	nd	nd	0.31	nd	0.46	0.50	0.58	-0.37	-0.03	0.30	nd	0.11	-0.02	0.55	0.61	0.23	-0.17	
	P	-0.10	0.00	0.15	-0.06	0.21	0.07	nd	0.19	nd	-0.01	-0.08	-0.05	nd	nd	nd	nd	0.06	nd	0.10	-0.07	-0.09	-0.07	-0.16	0.01	nd	-0.01	-0.05	0.14	-0.14	0.12	0.74	
5	H	0.63	0.10	0.14	0.80	0.09	-0.33	0.44	-0.34	nd	0.43	nd	-0.30	0.64	0.79	nd	nd	0.11	nd	0.72	0.56	0.82	-0.28	0.21	0.54	-0.11	-0.11	-0.15	0.21	0.76	-0.03	-0.11	
	T	0.13	0.34	0.42	0.02	-0.63	0.45	-0.25	nd	0.24	nd	-0.59	0.56	0.39	nd	nd	nd	0.20	nd	0.61	0.29	0.65	-0.40	0.37	0.55	-0.04	-0.04	-0.24	-0.01	0.61	-0.38	-0.10	
	P	0.02	0.03	0.21	-0.06	-0.08	-0.26	nd	-0.03	nd	-0.03	nd	-0.19	-0.11	0.11	nd	nd	-0.26	nd	-0.04	-0.01	-0.03	-0.15	-0.21	-0.05	-0.07	-0.09	-0.06	0.01	-0.09	-0.13	-0.08	
6	H	0.58	-0.14	0.64	0.37	0.65	0.69	0.26	0.50	0.91	-0.54	-0.42	-0.19	0.57	0.46	-0.60	0.60	0.79	0.59	0.73	0.91	0.88	0.84	-0.74	0.69	0.84	0.50	-0.22	-0.17	0.30	0.86	-0.26	-0.38
	T	0.10	0.48	0.26	0.23	0.38	0.26	0.12	0.64	-0.34	-0.33	-0.24	0.20	0.02	-0.65	0.28	0.40	0.45	0.40	0.62	0.62	0.69	0.53	-0.60	0.57	0.60	0.21	-0.09	-0.25	0.33	0.56	-0.02	-0.35
	P	-0.02	0.06	-0.09	0.01	0.20	-0.21	-0.10	-0.05	0.11	-0.05	0.11	-0.05	-0.09	-0.10	-0.08	-0.19	-0.13	-0.05	0.00	-0.12	-0.11	-0.14	0.01	-0.02	-0.14	-0.10	-0.04	-0.06	0.04	-0.10	-0.13	0.03

Note: Statistical significances ( $\alpha < 0.05$ ) were marked in bold and highlighted in grey; nd - lack of results due to not enough set of data necessary to perform the calculation.

et al., 2002; Dragon & Marciniak, 2010). Given the progressive warming of the Arctic climate and the sensitivity of permafrost catchments of Svalbard to changes in air temperature, it is impossible to ignore the impact of climate change on the hydrochemistry of such catchments. The layer of active permafrost in the study area can reach a thickness of more than 202 cm (Marsz et al., 2013). The study period coincided with the beginning of the ablation season (June/July) with some amounts of snow still accumulated in the depressions of the catchment and the mouth of the creek (Figure S1). The mean air temperature for the 2021 measurement period was the same as recorded at Calypsostranda in 2012 (4.88°C) (Table S2) (Lehmann-Konera et al., 2018) and lower than calculated for the multiannual observations 1986–2011 (5.0°C) (Mędrek et al., 2014) and observed in 2016 (5.0°C) (Lehmann-Konera et al., 2023). In terms of daily precipitation total, the study season 2021 was characterized by the lowest amount of precipitation (10.7 mm) (Figure S2) in comparison with the multiannual observations 1986–2011 (32.4 mm) (Mędrek et al., 2014), measurements noted in 2012 (26.4 mm) (Lehmann-Konera et al., 2018) and 2016 (46.7 mm) (Lehmann-Konera et al., 2023). The results of the correlation matrix (Tables 2 and 3) clearly indicate a strong relationship between an increase in average air temperature ( $T$ ) and a decrease in flow rate ( $Q$ ) in the surface water of the stream and the decrease in groundwater table (Figures S3 and S4). With a decrease in the groundwater level, the amount of water that feeds the surface water of the basin also decreases. Moreover, a thicker active layer contributes to an increase in its ability to store water resources (Lehmann-Konera et al., 2018; Stachniak et al., 2022), promoting a decrease in surface water alimentation, and explaining the lack of impact of precipitation on the hydrology of the catchment (Tables 2 and 3). Like in previous studies, discharge intensity in this catchment (Lehmann-Konera et al., 2018) results in lower  $pH$  and  $SEC$  in surface waters.

## 4.2 | Hydrochemical response of the creek

According to the literature, the key factors shaping water chemistry on Svalbard include dry and wet deposition of pollutants and rock-water interactions (Cooper et al., 2002; Dragon & Marciniak, 2010). It is worth noting that coastal areas, such as the Rensdyrbekken catchment, are strongly influenced by marine aerosols, which may be a source of  $Na$  as well as other trace elements (Kozioł et al., 2021; Lehmann-Konera et al., 2023; Szumińska et al., 2018). Chemical weathering is largely dependent on temperature (Cooper et al., 2002). Because the  $pH$  of surface water is neutral-light alkaline (Table 1), immobilization of elements and their strong binding to organic matter can occur (Kozak et al., 2016). Hence, in surface waters, the negative effect of an increase in  $Q$  on elements such as  $Ca$ ,  $K$ ,  $Li$ , and  $Mg$  is usually observed (Table 2), while an increase in  $pH$  and  $SEC$  is accompanied by an increased presence of these elements. The lowering of the water table in piezometers may occur during the season of thawing of the active layer, which constitutes a barrier to water runoff and migration of chemical compounds (Szumińska et al., 2023). In the case

of shallow groundwater in Rensdyrbekken (Figure S4) where lowering the water table results in increased chemical weathering processes, a positive correlation of  $H$  with both  $pH$  and  $SEC$  is observed (Table 3) which, depending on the geology of the measurement point, usually results in a positive correlation with elements due to reduced leaching of compounds from the active layer.

It is not the only process explaining strong correlations between average air temperature ( $T$ ) and an increase or decrease in element levels in both surface water and groundwater of the catchment (Tables 2 and 3). Additional factors include the phenomenon of biogeochemical “breathing” in soils (Chmiel et al., 2013). The catchment area of Rensdyrbekken is rich in brown soils abundant in organic matter and humus (Klimowicz et al., 2013). The presence of DOC in stream water leads to changes in the hydrogeochemical cycle of trace elements through red-ox reactions as well as peptization and sorption processes (Kozak et al., 2016). It explains the negative correlations of DOC in surface water with individual elements (Table 2).

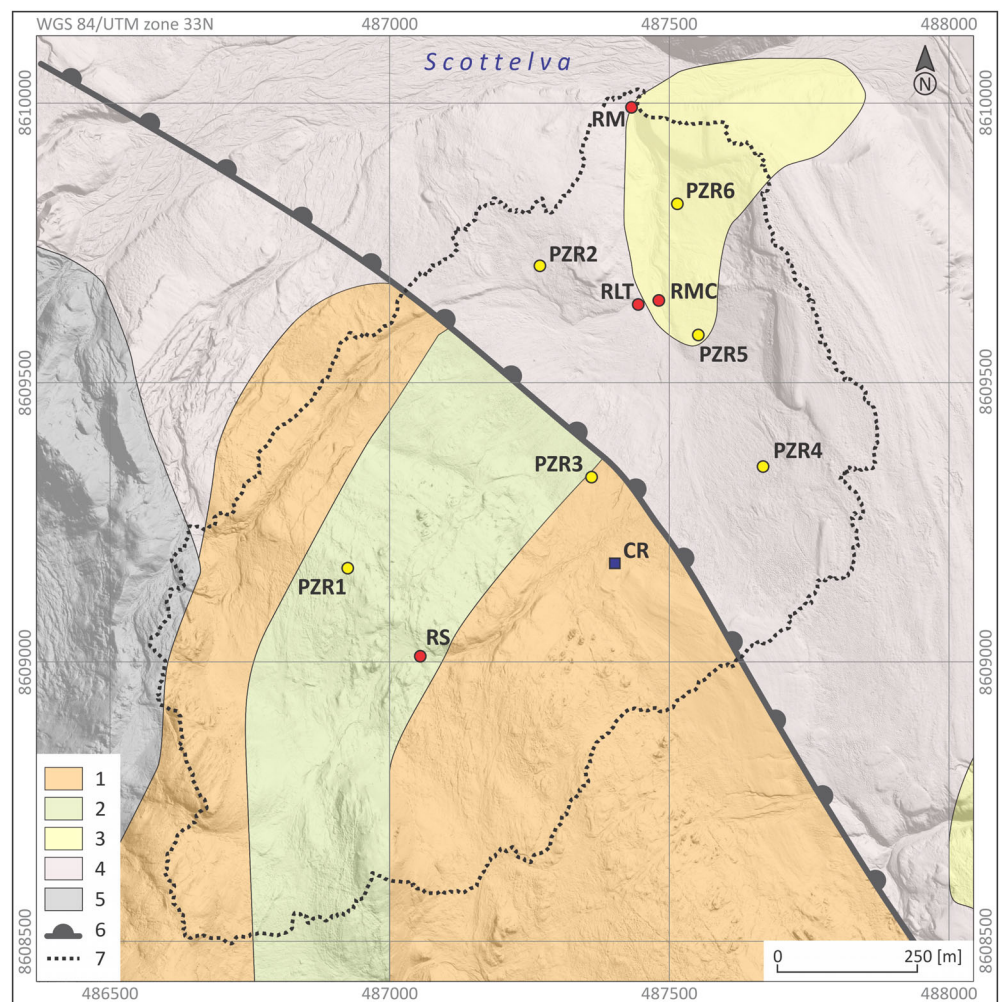
## 4.3 | Catchment geology

Regardless of the meteorological conditions and hydrology of the catchment, the rocks within which the catchment functions will have a decisive influence on the final amount of elements in the water. Figure 5 shows the location of the measurement points in separate geological formations, significantly affecting the water  $pH$ ,  $SEC$ , and concentrations of individual elements in various locations in the catchment. Therefore, the Bellsund Group formation with daimictite covers point PZR\_3, and the Bellsund phyllite PZR\_1 and RS. The remaining points lie behind the normal fault on tertiary formations (Birkenmajer, 2006). PZR\_5 and 6 and RMC lie within the Calypsostranda Group formation rich in sandstone, siltstone, shale, and coal. By contrast, PZR\_2 and 4 and RLT lie within marine deposits. The RM section lies on the border of the Calypsostranda Group and marine deposits.

In studied waters, significant levels of  $Ca$  and  $Mg$  (Table 1) may be resulted by considerable share of calcite and dolomite in mineral composition of rocks of Bohlinryggen, to which the upper part of catchment belongs (Chmiel et al., 2009). These compounds were indicated as geologically originated in waters of studied area (Chmiel et al., 2013; Szumińska et al., 2018). The other highly represented rocks derived elements, such as  $K$ ,  $Al$ , and  $Fe$ , may be the product of aluminosilicates weathering. Furthermore,  $Fe$  and  $Al$  is highly represented in study area (Chmiel et al., 2009) and also relatively easily soluble from moraine deposits (Szopińska et al., 2018). These elements are grouped as the one of main clusters in the river mouth (RM\_C2) and selected groundwaters (PZR\_1-C2, PZR\_4-C1, and P\_ZR\_6-C1) (Figure 4). In the previous study, also  $Sr$  (associated with mentioned above clusters in this study) were recognized as the rocks derived element (Szumińska et al., 2018).  $Na$ , which is as well highly represented in studied waters (Table 1), may be associated with both atmospheric and rocks sources. Furthermore, domination of unconsolidated marine deposits in the lower part of the catchment, supported leaching of



**FIGURE 5** Map of geological (Source: offline Geological Map of Svalbard, scale 1:75000; NPI 2016): Geological unit: 1. Bellsund Group—undifferentiated (a. lithology: diamictite; b. age period: Cryogenian and/or Ediacaran); 2. Bellsund phyllite unit (a. lithology: phyllite with clasts; b. age period: Cryogenian and/or Ediacaran); 3. Calypsostranda Group (a. lithology: sandstone, siltstone, shale, coal; b. age period: late Eocene—early Oligocene); 4. marine deposit—unconsolidated (a. lithology: marine deposit; b. age period: Holocene); 5. moraine—unconsolidated (a. lithology: moraine; b. age period: Holocene); 6. normal fault; 7. catchment border. [Colour figure can be viewed at [wileyonlinelibrary.com](http://wileyonlinelibrary.com)]



elements during active layer thawing and resulted relatively high  $\sum TE$  (Figure 3). Extremely high values of  $\sum TE$ , Ca, K, Li, Mg, and Na in PZR\_6 coupled with the high DOC level may be the result of the occurrence of silt stones, sandstones, shales, and coal in this site (Figures 4 and 5).

In studied catchment geological conditions, soils features (depth, moisture, grain-size matrix) and changing depth of water level influence potential leaching of elements into water. At the beginning of studied period, the water depth in piezometers not exceed 10 cm b.g.l. and increased until the end of July to 60–80 cm b.g.l. in the mot sites excluding PZR\_3, where not exceed 30 cm b.g.l. (Figure S4). Therefore, share of atmospheric compounds (dry and wet deposition) vs geological derived compounds could change during progressive seasonal permafrost thawing.

## 5 | CONCLUSIONS

Interdisciplinary studies of the permafrost catchment of the west coast of Bellsund have shown a strong influence of an increase in mean air temperature on the hydrological and geochemical processes shaping the chemistry of both surface water and groundwater functioning within the study catchment. Compared with previous research

seasons, the mean air temperature recorded on Calypsostranda in 2021 did not differ significantly. The situation was different in the case of the total daily precipitation. The 2021 study season was significantly drier in comparison with the previous ones in 2012 and 2016, which resulted in reduced leaching of DOC and elements from the well-developed drainage system in the soil formations of the Rensdyrbekken catchment. In the context of the ongoing climate change and an increase in average air temperature, a significant decrease in the level of the groundwater table of the coast of eastern Svalbard can be expected. In the worst-case scenario, it could result in the disappearance of watercourses fed by the thawing of the permafrost in these areas. Large-scale hydrogeochemical studies have shown great variations between the elemental composition of surface water and shallow groundwater on Svalbard even between measurement points within the same geological formations. This study also confirmed the dominant role of rock-water interaction processes as an important aspect in shaping water chemistry in permafrost catchments of the west coast of Svalbard.

## AUTHOR CONTRIBUTIONS

S.L.K. involved in conceptualization; S.L.K. and Ž.P. involved in methodology; P.Z., M.F. and Ł.F., M.D. involved in validation; P.Z., K.R., and R.A. involved in formal analysis; S.L.K., P.Z., M.F., Ł.F.,

and K.N. involved in investigation; S.L.K., P.Z., M.F., and Ż.P. involved in resources; S.L.K., P.Z., K.R., and M.F. involved in data curation; S.L.K., P.Z., Ł.F., K.R., M.D., and D.S. involved in writing—original draft preparation; S.L.K., M.R., R.B., P.Z., K.R., D.S., and Ż.P. involved in writing—review and editing; S.L.K., P.Z., Ł.F., K.R., R.B., M.R., and Ż.P. involved in visualization; S.L.K. and Ż.P. involved in supervision; S.L.K. involved in project administration; S.L.K. involved in funding acquisition; all authors have read and agreed to the published version of the manuscript.

## ACKNOWLEDGMENTS

This research was funded by the National Science Centre of Poland, grant number 2019/32/C/ST10/00483. The research activities co-financed by the funds granted under the Research Excellence Initiative of the University of Silesia in Katowice. Special thanks are due for Ewa Formela from the Gdańsk University for her great contribution and assistance in the analysis of DOC in freshwater samples.

## CONFLICT OF INTEREST STATEMENT

There is no conflict of interest.

## DATA AVAILABILITY STATEMENT

The data that support the findings of this study are available from the corresponding author upon reasonable request.

## ORCID

Sara Lehmann-Konera  <https://orcid.org/0000-0002-8318-0224>

Piotr Zagórski  <https://orcid.org/0000-0002-6086-0470>

Krzysztof Raczynski  <https://orcid.org/0000-0002-2098-4292>

Marcin Frankowski  <https://orcid.org/0000-0001-6315-3758>

Łukasz Franczak  <https://orcid.org/0000-0002-7358-5658>

Mateusz Dobek  <https://orcid.org/0000-0001-5614-436X>

Danuta Szumińska  <https://orcid.org/0000-0001-7142-9080>

Marek Ruman  <https://orcid.org/0000-0001-9424-7589>

Ramia Al Bakain  <https://orcid.org/0000-0003-0419-0828>

Żaneta Polkowska  <https://orcid.org/0000-0002-2730-0068>

## REFERENCES

- Abbott, B. W., Jones, J. B., Godsey, S. E., Larouche, J. R., & Bowden, W. B. (2015). Patterns and persistence of hydrologic carbon and nutrient export from collapsing upland permafrost. *Biogeosciences*, 12, 3725–3740. <https://doi.org/10.5194/bg-12-3725-2015>
- AMAP. (2012). AMAP. SWIPA 2011 Overview Report. Arctic climate issues 2011: Changes in Arctic snow, water, ice and permafrost/Arctic Monitoring and Assessment Programme (AMAP), Oslo.
- Birkenmajer K. (2006). Character of basal and intraformational unconformities in the Calypsostranda Group (late Palaeogene), Bellsund, Spitsbergen Basal unconformity of the Calypsostranda Group at Skilvika 27. 107–118.
- Biskaborn, B. K., Smith, S. L., Noetzi, J., Matthes, H., Vieira, G., Streletskiy, D. A., Schoeneich, P., Romanovsky, V. E., Lewkowicz, A. G., Abramov, A., Allard, M., Boike, J., Cable, W. L., Christiansen, H. H., Delaloye, R., Diekmann, B., Drozdov, D., Etzelmüller, B., Grosse, G., ... Lantuit, H. (2019). Permafrost is warming at a global scale. *Nature Communications*, 10, 264. <https://doi.org/10.1038/s41467-018-08240-4>
- Carey, S. K. (2003). Dissolved organic carbon fluxes in a discontinuous permafrost subarctic alpine catchment. *Permafrost and Periglacial Processes*, 14, 161–171. <https://doi.org/10.1002/ppp.444>
- Chmiel S, Bartoszewski S, Michalczyk Z. (2013). Hydrochemistry. 102–117.
- Chmiel, S., Reszka, M., & Rysiak, A. (2009). Heavy metals and radioactivity in environmental samples of the Scott glacier region on Spitsbergen in summer 2005. *Quaestiones Geographicae*, 28A(1), 23–29.
- Christiansen, H. H., Gilbert, G. L., Demidov, N., Guglielmin, M., Isaksen, K., Osuch, M., & Boike, J. (2018). Permafrost thermal snapshot and active-layer thickness in Svalbard. The State of Environmental Science in Svalbard – an annual report.
- Christiansen, H. H., Gilbert, G. L., Neumann, U., Demidov, N., Guglielmin, M., Isaksen, K., Osuch, M., & Boike, J. (2020). SESS report 2020 – the state of environmental science in Svalbard – an annual report, Svalbard integrated Arctic earth observing system, Longyearbyen. Ground ice content, drilling methods and equipment and permafrost dynamics in Svalbard 2016–2019 (PermaSval), Longyearbyen. <https://doi.org/10.5281/zenodo.4294095>
- Cooper, R. J., Wadham, J. L., Tranter, M., Hodgkins, R., & Peters, N. E. (2002). Groundwater hydrochemistry in the active layer of the proglacial zone, Finsterwalderbreen, Svalbard. *Journal of Hydrology*, 269, 208–223. [https://doi.org/10.1016/S0022-1694\(02\)00279-2](https://doi.org/10.1016/S0022-1694(02)00279-2)
- Dolnicki, A. P., Grabiec, M., Puczko, D., Gawor, Ł., Dolnicki, P., Grabiec, M., Puczko, D., & Gawor, Ł. (2013). Title: Variability of temperature and thickness of permafrost active layer at coastal sites of Svalbard Budzik, Jan Klementowski Citation Style: Dolnicki Piotr, Grabiec Mariusz, Puczko Dariusz, Gawor Łukasz, Budzik Tomasz, Klementowski Jan, 34. <https://doi.org/10.2478/popore>
- Dragon, K., & Marciniak, M. (2010). Chemical composition of groundwater and surface water in the Arctic environment (Petuniabukta region, central Spitsbergen). *Journal of Hydrology*, 386, 160–172. <https://doi.org/10.1016/j.jhydrol.2010.03.017>
- Dragon, K., Marciniak, M., Szpikowska, G., & Wawrzyniak, T. (2015). The hydrochemistry of glacial Ebba River (Petunia Bay, Central Spitsbergen): Groundwater influence on surface water chemistry. *Journal of Hydrology*, 529, 1499–1510. <https://doi.org/10.1016/j.jhydrol.2015.08.031>
- Hanssen-Bauer, I., Førland, E. J., Hisdal, H., Mayer, S., Sandø, A. B., Sorteberg, A., Adakudlu, M., Andresen, J., Bakke, J., Beldring, S., Benestad, R., Bilt, W., Bogen, J., Borstad, C., Breili, K., Breivik, Ø., Børsheim, K. Y., Christiansen, H. H., Dobler, A., ... Wong, W. K. (2019). Climate in Svalbard 2100.
- Harasimiuk, M., & Gajek, G. (2013). Tectonic and lithology. In P. Zagórski, M. Harasimiuk, & J. Rodzik (Eds.), *The geographical environment of W part of wedel Jarlsberg land (Spitsbergen, Svalbard)* (pp. 34–47). UMCS.
- Humlum, O., Instanes, A., & Sollid, J. L. (2003). Permafrost in Svalbard: A review of research history, climatic background and engineering challenges. *Polar Research*, 22, 191–215. <https://doi.org/10.1111/j.1751-8369.2003.tb00107.x>
- Klimowicz, Z., Melke, J., & Chodorowski, J. (2013). In P. Zagórski (Ed.), *Soils* (pp. 248–271). UMCS.
- Kozak, K., Koziol, K., Luks, B., Chmiel, S., Ruman, M., Marć, M., Namieśnik, J., & Polkowska, Ż. (2015). The role of atmospheric precipitation in introducing contaminants to the surface waters of the faglebekken catchment, spitsbergen. *Polar Research*, 34, 24207–24216. <https://doi.org/10.3402/polar.v34.24207>
- Kozak, K., Polkowska, S., Luks, B., Chmiel, S., Ruman, M., Lech, D., Koziol, K., Tsakovski, S., & Simeonov, V. (2016). Arctic catchment as a sensitive indicator of the environmental changes: Distribution and migration of metals (Svalbard). *International Journal of Environmental Science and Technology*, 13, 2779–2796. <https://doi.org/10.1007/s13762-016-1137-6>
- Kozak, K., Ruman, M., Kosek, K., Karasiński, G., Stachnik, Ł., & Polkowska, Z. (2017). Impact of volcanic eruptions on the occurrence

- of PAHs compounds in the aquatic ecosystem of the southern part of West Spitsbergen (Hornsund Fjord, Svalbard). *Water*, 9, 42–62. <https://doi.org/10.3390/w9010042>
- Kozioł, K., Uszczyk, A., Pawlak, F., Frankowski, M., & Polkowska, Ż. (2021). Seasonal and spatial differences in metal and metalloid concentrations in the snow cover of Hansbreen, Svalbard. *Frontiers in Earth Science*, 8, 538762. <https://doi.org/10.3389/feart.2020.538762>
- Kristensen L. (2008). Temperatures in coastal permafrost in the Svea area, Svalbard temperature measurements in boreholes. Ninth International Conference on Permafrost 1005–1010.
- Kwok, K. Y., Yamazaki, E., Yamashita, N., Taniyasu, S., Murphy, M. B., Horii, Y., Petrick, G., Kallerborn, R., Kannan, K., Murano, K., & Lam, P. K. S. (2013). Transport of perfluoroalkyl substances (PFAS) from an arctic glacier to downstream locations: Implications for sources. *Science of the Total Environment*, 447, 46–55. <https://doi.org/10.1016/j.scitotenv.2012.10.091>
- Lantuit, H., Overduin, P. P., & Wetterich, S. (2013). Recent progress regarding permafrost coasts. *Permafrost and Periglacial Processes*, 24, 120–130. <https://doi.org/10.1002/ppp.1777>
- Larouche, J. R., Abbott, B. W., Bowden, W. B., & Jones, J. B. (2015). The role of watershed characteristics, permafrost thaw, and wildfire on dissolved organic carbon biodegradability and water chemistry in Arctic headwater streams. *Biogeosciences*, 12, 4221–4233. <https://doi.org/10.5194/bg-12-4221-2015>
- Lehmann-Konera, S., Franczak, Ł., Kociuba, W., Szumi, D., & Polkowska, Ż. (2018). Comparison of hydrochemistry and organic compound transport in two non-glaciated high Arctic catchments with a permafrost regime (Bellsund Fjord, Spitsbergen). *Science of the Total Environment*, 614, 1037–1047. <https://doi.org/10.1016/j.scitotenv.2017.09.064>
- Lehmann-Konera, S., Kociuba, W., & Franczak, Ł. (2019). Concentrations and loads of DOC, phenols and aldehydes in a proglacial arctic river in relation to hydro-meteorological conditions. A case study from the southern margin of the Bellsund Fjord – SW Spitsbergen. *Catena*, 174, 117–129. <https://doi.org/10.1016/j.catena.2018.10.049>
- Lehmann-Konera S, Kociuba W, Franczak Ł, Polkowska Ż. (2021). Effects of biotransport and hydro-meteorological conditions on transport of trace elements in the Scott River (Bellsund, Spitsbergen). 1–21. <https://doi.org/10.7717/peerj.11477>
- Lehmann-Konera, S., Ruman, M., Franczak, Ł., & Polkowska, Z. (2020). Contamination of arctic lakes with persistent toxic pah substances in the NW part of wedel Jarlsberg land (Bellsund, Svalbard). *Water*, 12, 411–425. <https://doi.org/10.3390/w12020411>
- Lehmann-Konera, S., Ruman, M., Frankowski, M., Matarzewski, Ł., Raczyński, K., Pawlak, F., Kozioł, K., & Polkowska, Ż. (2023). Rainwater chemistry composition in Bellsund: Sources of elements and deposition discrepancies in the coastal area (SW Spitsbergen, Svalbard). *Chemosphere*, 313, 137281. <https://doi.org/10.1016/j.chemosphere.2022.137281>
- Marsz, A. A., Styszyńska, A., Pekala, K., & Repelewska-Pekalowa, J. (2013). Influence of meteorological elements on changes in active-layer thickness in the Bellsund region, Svalbard. *Permafrost and Periglacial Processes*, 24, 304–312. <https://doi.org/10.1002/ppp.1790>
- Mędrek, K., Gluza, A., Siwek, K., & Zagórski, P. (2014). The meteorological conditions on the Calypsobyen in summer 2014 on the background of multiyear 1986–2011. Polish: Warunki meteorologiczne na stacji w Calypsobyen w sezonie letnim 2014 na tle wielolecia 1986–2011. *Problemy Klimatologii Polarnej*, 24, 37–50.
- Olichwer, T., Tarka, R., & Modelska, M. (2013). Chemical composition of groundwaters in the Hornsund region, southern Spitsbergen. *Hydrology Research*, 44, 117–130. <https://doi.org/10.2166/nh.2012.075>
- Petrone, K. C., Jones, J. B., Hinzman, L. D., & Boone, R. D. (2006). Seasonal export of carbon, nitrogen, and major solutes from Alaskan catchments with discontinuous permafrost. *Journal of Geophysical Research: Biogeosciences*, 111, 1–13. <https://doi.org/10.1029/2005JG000055>
- Polkowska, Z., Cichala-Kamrowska, K., Ruman, M., Kozioł, K., Krawczyk, W. E., & Namieśnik, J. (2011). Organic pollution in surface waters from the Fuglebekken basin in Svalbard, Norwegian Arctic. *Sensors*, 11, 8910–8929. <https://doi.org/10.3390/s110908910>
- Stachniak, K., Sitek, S., Ignatiuk, D., & Jania, J. (2022). Hydrogeological model of the Forefield drainage system of Werenskiöldbreen, Svalbard. *Water*, 14, 1514–1536. <https://doi.org/10.3390/w14091514>
- Stachnik, L., Majchrowska, E., Yde, J. C., Nawrot, A. P., Cichała-Kamrowska, K., Ignatiuk, D., & Piechota, A. (2016). Chemical denudation and the role of sulfide oxidation at Werenskiöldbreen, Svalbard. *Journal of Hydrology*, 538, 177–193. <https://doi.org/10.1016/j.jhydrol.2016.03.059>
- Stachnik, Ł., Yde, J. C., Nawrot, A., Uzarowicz, Ł., Łepkowska, E., & Kozak, K. (2019). Aluminium in glacial meltwater demonstrates an association with nutrient export (Werenskiöldbreen, Svalbard). *Hydrological Processes*, 33, 1638–1657. <https://doi.org/10.1002/hyp.13426>
- Szopińska, M., Szumińska, D., Bialik, R. J., Chmiel, S., Plenzler, J., & Polkowska, Ż. (2018). Impact of a newly-formed periglacial environment and other factors on fresh water chemistry at the western shore of Admiralty Bay in the summer of 2016 (King George Island, maritime Antarctica). *Science of the Total Environment*, 613, 619–634. <https://doi.org/10.1016/j.scitotenv.2017.09.060>
- Szumińska, D., Kozioł, K., Chalov, S. R., Efimov, V. A., Frankowski, M., Lehmann-Konera, S., & Polkowska, Ż. (2023). Reemission of inorganic pollution from permafrost?—a freshwater hydrochemistry study in the lower Kolyma basin (north-East Siberia). *Land Degradation and Development*, 1–15, 5591–5605. <https://doi.org/10.1002/ldr.4866>
- Szumińska, D., Szopińska, M., Lehmann-Konera, S., Franczak, Ł., Kociuba, W., Chmiel, S., Kalinowski, P., & Polkowska, Ż. (2018). Water chemistry of tundra lakes in the periglacial zone of the Bellsund fiord (Svalbard) in the summer of 2013. *Science of the Total Environment*, 624, 1669–1679. <https://doi.org/10.1016/j.scitotenv.2017.10.045>
- Wadham, J. L., Cooper, R. J., Tranter, M., & Bottrell, S. (2007). Evidence for widespread anoxia in the proglacial zone of an Arctic glacier. *Chemical Geology*, 243, 1–15. <https://doi.org/10.1016/j.chemgeo.2007.04.010>
- Wawrzyniak, T., & Osuch, M. (2020). A 40-year high Arctic climatological dataset of the polish Polar Station Hornsund (SW Spitsbergen, Svalbard). *Earth System Science Data*, 12, 805–815. <https://doi.org/10.5194/essd-12-805-2020>
- White, D., Hinzman, L., Alessa, L., Cassano, J., Chambers, M., Falkner, K., Francis, J., Gutowski, W. J., Holland, M., Holmes, R. M., Huntington, H., Kane, D., Kliskey, A., Lee, C., McClelland, J., Peterson, B., Rupp, T. S., Straneo, F., Steele, M., ... Zhang, T. (2007). The arctic freshwater system: Changes and impacts. *Journal of Geophysical Research: Biogeosciences*, 112, 1–21. <https://doi.org/10.1029/2006jg000353>

## SUPPORTING INFORMATION

Additional supporting information can be found online in the Supporting Information section at the end of this article.

**How to cite this article:** Lehmann-Konera, S., Zagórski, P., Nowiński, K., Raczyński, K., Frankowski, M., Franczak, Ł., Dobek, M., Szumińska, D., Ruman, M., Al Bakain, R., & Polkowska, Ż. (2024). Spatial variability of the hydrochemistry of shallow groundwaters and surface waters of the Rensdyrbekken: A case study of a permafrost catchment in Bellsund (SW Spitsbergen, Svalbard). *Land Degradation & Development*, 35(5), 1874–1887. <https://doi.org/10.1002/ldr.5028>